2013

Scaling Normal Adhesion Force Capacity with a Generalized Parameter

Michael D. Bartlett, *University of Massachusetts - Amherst*
Alfred J. Crosby, *University of Massachusetts - Amherst*

Langmuir

Article

pubs.acs.org/Langmuir

Scaling Normal Adhesion Force Capacity with a Generalized Parameter

Michael D. Bartlett and Alfred J. Crosby*

Polymer Science and Engineering, University of Massachusetts Amherst, 120 Governors Drive, Amherst, Massachusetts 01003, United States

Supporting Information

ABSTRACT: The adhesive response of a rigid flat cylindrical indenter in contact with a compliant elastic layer of varying confinement is investigated experimentally and described analytically. Using a soft elastic gel with substrate thickness, t, and indenter radius, a, 28 unique combinations of the confinement parameter, a/t, are examined over a range of $0.016 < a/t < 7.2$. Continuous force capacity predictions as a function of a/t and material properties are provided through a scaling theory and are found to agree well with the experimental data. We further collapse all of the data over orders of magnitude in adhesive force capacity onto a single line described by a generalized reversible adhesion scaling parameter, A/C, where A is the contact area and C is the compliance. As the scaling analysis does not assume a specific separation mechanism the adhesive force capacity is well described during both axisymmetric edge separation and during interfacial fingering and cavitation instabilities. We discuss how the geometry of the contact, specifically increasing the degree of confinement, allows reversible adhesive materials to be designed that are not "sticky" or "tacky", yet can be very strong and provide high performance.

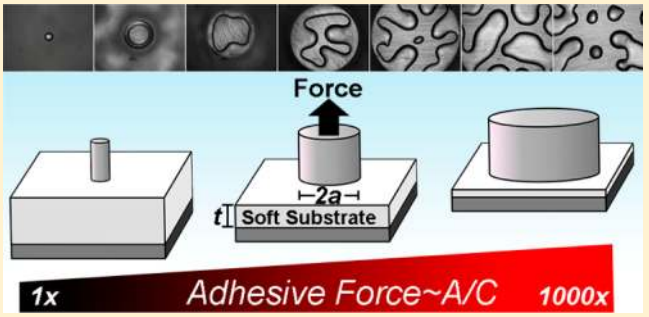

INTRODUCTION

The adherence of a flat punch to a soft, thin layer is important in many different fields across a wide range of length scales, such as the adhesion of barnacles to ship hulls, pressure sensitive adhesives and micro contact printing.[1−6] The mechanical and adhesive response of materials of finite thickness are not only dependent on material properties, but can also strongly depend on the geometry of the contact. Specifically, as the punch radius, a, becomes commensurate or larger than the soft layer thickness, t, the system becomes laterally constrained, resulting in a different mechanical behavior relative to a bulk sample. The degree of this constraint is described by the dimensionless a/t confinement parameter. The importance of the a/t ratio has been demonstrated in numerous adhesive systems, from soft planar layers to gecko-inspired fibrillar systems, and can have a dramatic affect on adhesive performance.[7−10] The a/t ratio has also been shown to modify the stress distribution under the rigid punch, which can significantly change the deformation behavior and debonding mechanisms of the compliant layer.[11−13] Most mechanical or adhesive predictions of these interfaces have focused discretely on either nonconfined or highly confined systems[14−20] or on the observed debonding morphologies such as interfacial or bulk cavitation and fingering instabilities.[9,11,21−24] These analyses have generally focused on debonding mechanisms related to energy dissipation and the energy release rate. This has provided critical insight into the design of viscoelastic, pressure sensitive adhesives, where the separation energy is a primary descriptor of performance. In the context of elastic, reversible adhesive systems, where significant energy dissipation and specific interfacial chemistries are not a strongly tunable parameter, performance is described by the force required to separate the interface.

Previously, Kendall used a fracture mechanics energy balance to determine the adhesive force capacity, or pull-off force, F_C, of a rigid cylindrical punch adhered to an elastic layer in two extremes.[14] The first for a compliant layer of infinite thickness where F_C is independent of t and scales as $a^{3/2}$, and the second in a highly confined regime where F_C scales as $a^2/t^{1/2}$. More detailed theoretical analyses have been performed by Yang and Li, but again analytical F_C predictions were only provided for unconfined or highly confined layers.[18] These works demonstrated that F_C is very sensitive to lateral constraints, where drastically different behavior is observed for extreme values of a/t. However, predictions and experimental investigation of compliance and adhesive force capacity across a wide, continuous range of a/t ratios still requires further investigation.

In this work we utilize an elastic, reversibly adhesive swollen gel and investigate the mechanical and adhesive behavior by varying the radius of the rigid punch indenter and substrate thickness. To describe the adhesive force capacity, we use our

Received: April 10, 2013
Revised: June 27, 2013
Published: August 7, 2013

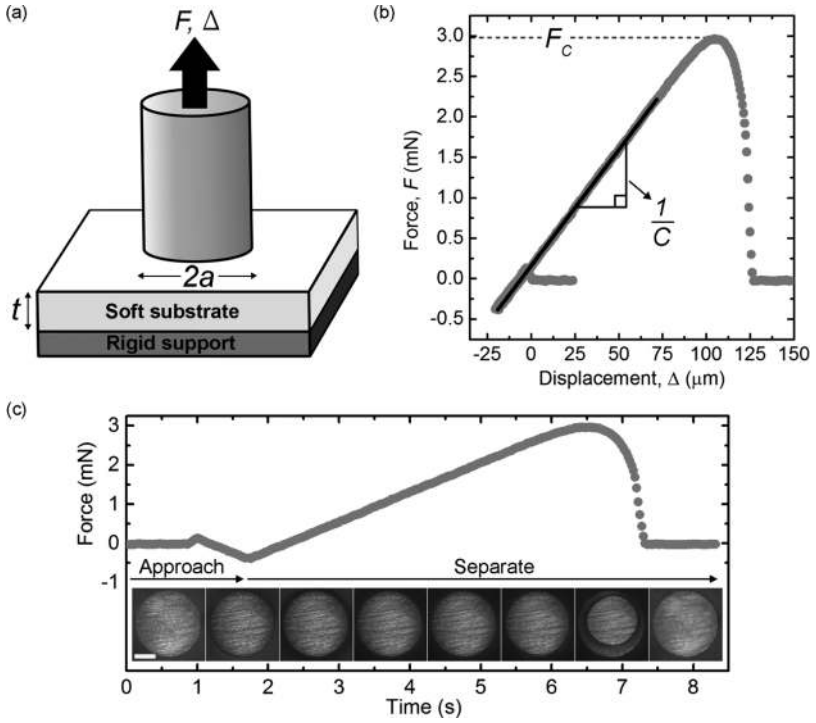

Figure 1. (a) Schematic of the experimental set up where a cylindrical punch of radius a is brought into contact with a soft substrate of thickness t. After contact is obtained, the punch is retracted until the interface separates. (b) Experimental data showing a typical force versus displacement plot (a = 0.75 mm, t = 3.2 mm), negative force values are compressive and positive are tensile. The compliance, C, is the inverse of the slope of the curve from the maximal compressive preload to 75% of the maximal tensile load, and upon reaching a critical adhesive force capacity, F_C, the interface fails. (c) Force versus time data of the experimental data in (b) and contact images during the experiment (scale bar = 500 μm), which show the punch obtains full contact, and upon reaching F_C the interface separates radially inward.

recently developed scaling argument, which has been shown to provide a consistent understanding in reversible adhesive systems.[25,26] Within this framework, we predict the contact compliance and adhesive force capacity over orders of magnitude in the a/t ratio through a continuous function. The implications of these results are discussed in the context of material testing and adhesive design. The adhesive force capacity data is then collapsed onto a single line described by our reversible adhesion scaling parameter. This analysis demonstrates the versatility of this scaling relationship to describe adhesive force capacity under normal loading conditions in both nonconfined and confined systems through a wide range of contact sizes and geometries.

EXPERIMENTAL SECTION

Material Fabrication. A highly elastic, thermoreversible gel consisting of a poly(methyl methacrylate)-poly(*n*-butyl acrylate)-poly(methyl methacrylate) [PMMA-PnBA-PMMA] triblock copolymer swollen with 2-ethylhexanol is used as the compliant substrate. The triblock copolymer was kindly provided by Kuraray Co. Ltd., where the PMMA end-blocks have a molecular weight of 25 000 g mol^{-1} and the PnBA midblock has a molecular weight of 116 000 g mol^{-1}. To fabricate the substrate a 15 wt % solution of the triblock is dissolved at a temperature of 60 °C for 2 h. At this temperature the PMMA and PnBA blocks are both soluble in the solvent. The solution is then cast into glass molds of controlled depth on a hot plate, which is then moved onto a level surface to cool to room temperature (~20 °C). Upon cooling the PMMA end blocks become insoluble, forming micelles which are physically linked by the PnBA midblocks.[15,27] The thickness of the compliant substrate is measured by bringing a probe attached to a nanopositioner into contact with the surface while monitoring the displacement from the supporting substrate.

Adhesion Characterization. The adhesion force-displacement relationships between the compliant substrate and rigid punch were measured using a custom built contact adhesion instrument and an Instron 5500R. The contact adhesion instrument consists of a rigid cylindrical punch attached to a load cell which is connected to a piezo-controlled linear actuator (Burleigh Inchworm nanopositioner) all of which is mounted over an inverted microscope (Zeiss Axiovert 200M).[28] The compliant substrate is positioned between the microscope and rigid punch. The rigid punches were fabricated from hardened steel rods (McMaster-Carr), which were cut and planarized with a grinding wheel and subsequently smoothed with polishing paper to a RMS roughness of less than 100 nm measured across lateral dimensions on the order of the punch diameter. Seven different sized punches with radii from 0.17 to 3.83 mm and four substrate thicknesses (0.53, 1.4, 3.2, 10.6 mm) were used for testing. For highly confined systems, the substrate stiffness increases rapidly and the adhesion measurements were performed on an Instron 5500R to ensure the instrument stiffness was at least 9× the substrate stiffness. Both instruments utilized a tilt and rotation platform (Newport) to adjust parallelism between the substrate and rigid punch to ensure reproducible results.[29]

The adhesion experiments were performed by bringing the punch into contact with the substrate at a displacement rate of 25 μm/s until a maximum compressive preload, and then retracted until complete separation occurred. Depending on the punch radius, the compressive preload ranged from 0.1 to 2.6 mN, while maintaining a preload to punch radius ratio of ~0.65 mN/mm. Force, displacement, and contact area images were continuously monitored and collected throughout the experiments with a custom computer program (National Instruments Labview), as seen in Figure 1. Each experiment was cycled at the same location on the substrate five times and was then analyzed with custom MATLAB code to measure compliance and force capacity. As previously reported, these gels are elastic, incompressible and the critical strain energy release rate is relatively insensitive to crack velocity.[15] Our results are consistent with this

dx.doi.org/10.1021/la4013526 | *Langmuir* 2013, 29, 11022−11027

previous work as adhesive force capacity was found to be independent of compressive preload and displacement rate for the range examined (Supporting Information, Figure S1).

RESULTS AND DISCUSSION

To describe the force capacity for a rigid cylindrical punch adhered to an elastic layer, we apply our previously developed adhesion scaling theory.[25,26] We consider that an adhesive joint of contact area (A) loaded through a force (F) will completely separate upon reaching a critical force capacity (F_C). The elastic energy stored at the interface is primarily recovered by breaking and forming new surface contacts, such that inelastic processes are minimized. Within this framework, the adhesive force capacity (F_C) can be written as

$$F_C \sim \sqrt{G_C}\sqrt{\frac{A}{C}} \tag{1}$$

where C is the compliance in the loading direction and G_C is the critical strain energy release rate, which is set by the interfacial materials. As the derivation of this relationship did not assume a specific loading condition, geometry, or contact size, it serves as a general descriptor for reversible adhesive systems. Equation 1 will be the foundation for our investigation of reversible adhesion under normal loading conditions, where the force capacity will be described as a function of the a/t confinement parameter and more generally as the A/C scaling parameter.

To investigate contact compliance and adhesive force capacity, seven different punch radii ranging from 0.17 to 3.83 mm were evaluated on four different substrate thicknesses, providing 28 unique a/t combinations over a range of $0.016 < a/t < 7.2$. During the experiments, the punch was brought into contact with the substrate until a programmed maximum compressive preload and then retracted until complete separation occurred, as seen in Figure 1. The compliance was calculated from the experimental data by taking the inverse of the slope from the maximum compressive preload to $0.75F_C$, where F_C was taken as the maximum tensile force.

As Figure 2a demonstrates, C and F_C both vary when the contact radius a is changed while maintaining a constant thickness t. To specifically describe the compliance of a rigid, circular punch in contact with a soft, incompressible substrate of elastic modulus E, Shull et al. have shown a semiempirical model, which is written as[30]

$$C = \frac{3}{8Ea}\left[1 + 1.33\frac{a}{t} + 1.33\left(\frac{a}{t}\right)^3\right]^{-1} \tag{2}$$

The relationship shows that at low degrees of confinement the contribution from the a/t terms will be minimal, and the compliance reduces to a function of the material's elastic modulus and the contact radius, independent of thickness. As the degree of confinement increases, the compliance decreases and becomes a function of the confinement parameter. To investigate the deformation dependence on confinement we plot Ca versus a/t as seen in Figure 2b. Qualitatively, we see that at low degrees of confinement the compliance behavior is independent of the a/t ratio; however, as confinement is increased, the compliance begins to decrease and then decreases more rapidly as a/t is further increased. This behavior is quantitatively captured by eq 2, which provides a continuous prediction of the compliance of the contact. This

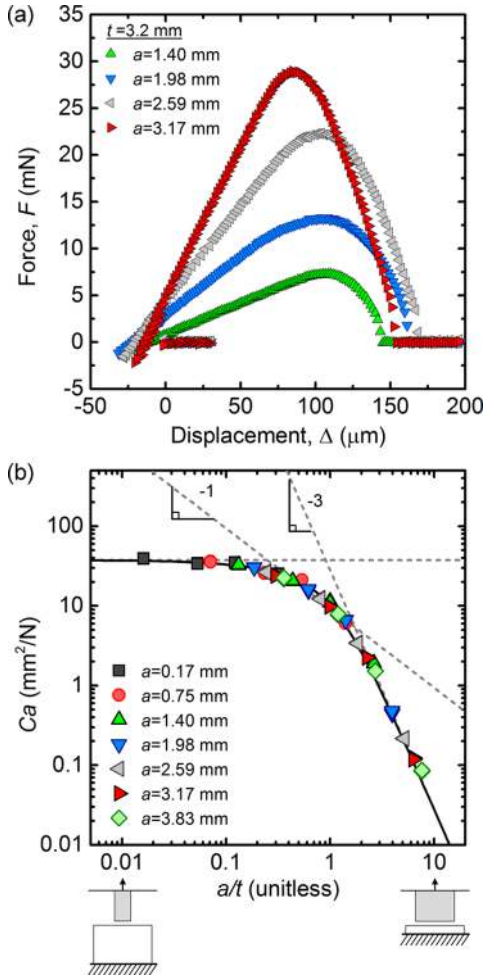

Figure 2. (a) Experimental data showing a force versus displacement plot for various punch radii at a constant substrate thickness of 3.2 mm, demonstrating a decrease in compliance as the punch radii is increased. (b) Log–log plot of Ca versus the confinement parameter a/t for seven different punch radii each evaluated on four different substrate thicknesses. The solid line represents the prediction of eq 2, with E = 10 kPa, and the dashed lines are guides to the eye.

data is fit with an elastic modulus of E = 10 kPa, which agrees with previously reported values of the triblock gel.[12]

To generate force capacity predictions as a function of specific geometric parameters, detailed expressions for A and C are substituted into eq 1. Upon substitution of eq 2 into eq 1 with a projected contact area $A = \pi a^2$,[7,8,15−17] the normalized force capacity scales as

$$\frac{F_C}{a^{3/2}} \sim \sqrt{G_C E}\sqrt{1 + 1.33\frac{a}{t} + 1.33\left(\frac{a}{t}\right)^3} \tag{3}$$

By plotting $F_C/a^{3/2}$ versus a/t, we see that eq 3 agrees with the experimental data as shown in Figure 3a. The equation demonstrates and our data confirms that for low values of a/t the adhesive force capacity is largely independent of substrate thickness or confinement. As the adhesive layer becomes confined, F_C increases as the a/t ratio increases. In the limits of unconfined and highly confined systems, eq 3 scales with a and t as previously described by Kendall, and Li and Yang, respectively.[14,18] In our experiments, the contact failed through axisymmetric radial crack growth ($a/t < 2.2$); however, as confinement increased, crack growth became irregular ($a/t >$

dx.doi.org/10.1021/la4013526 | Langmuir 2013, 29, 11022−11027

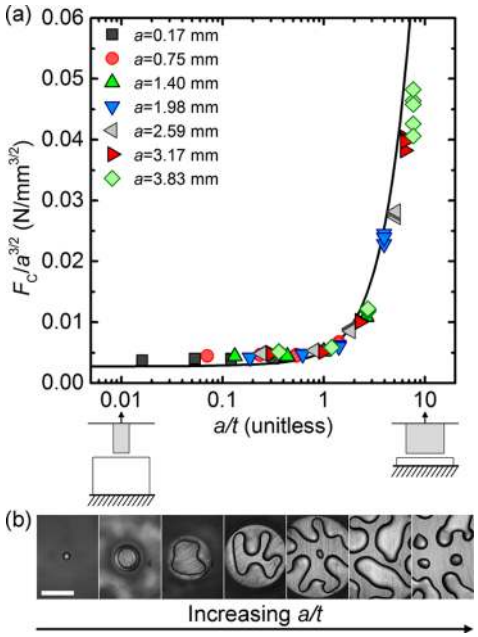

Figure 3. (a) Linear-log plot of normalized force capacity versus the confinement parameter a/t, for seven different punch radii each evaluated on four different substrate thicknesses, where the solid line represents eq 3, with E = 10 kPa and G_C = 0.05 J/m^2. (b) Contact images of the separation morphologies observed directly after F_C is achieved on the t = 0.53 mm substrate for all of the punches, with increasing punch radii from left to right, and confinement ratios ranging from 0.3 < a/t < 7.2 (scale bar = 2 mm).

2.2) and fingering instabilities were observed (a/t > 3.7). We note that at the highest degrees of confinement the theory is slightly overestimating the experimental data. This small difference in the predictions by eq 3 may be attributed to the emergence of interfacial fingering and cavitation instabilities (Figure 3b), which increase the contact compliance during separation and violate the circular contact geometry assumed in eq 2.[15] We anticipate that these instabilities may influence the details of the force capacity predictions in eq 3, but we expect F_C to increase as confinement is increased.

Equation 3 has important implications for both material testing and design. It demonstrates the need to know and control the a/t ratio during materials evaluation, where a small change in thickness for a given punch radius can have a dramatic effect on the measured adhesive performance. It also shows that adhesion can be enhanced, or a greater force capacity for a given contact radius, by reducing the compliant layer thickness and thus increasing the a/t ratio. This type of design could be used to make the force capacity of inherently "weak" adhesive materials with low G_C values, equal or greater than "strong" adhesive materials with high G_C values. Consider a "weak" adhesive with a low critical energy release rate of G_{CW} and confinement $(a/t)_W$ and a "strong" adhesive with G_{CS} and $(a/t)_S$. Equating the force capacities for a constant punch radii and elastic modulus of these two materials through eq 3 and solving in terms of the relative adhesive energy, G_{CS}/G_{CW}, we find:

$$\frac{G_{CS}}{G_{CW}} \sim \frac{1.33\left(\frac{a}{t}\right)_S^3 x^3 + 1.33\left(\frac{a}{t}\right)_S x + 1}{1.33\left(\frac{a}{t}\right)_S^3 + 1.33\left(\frac{a}{t}\right)_S + 1} \quad (4)$$

where x is the relative degree of confinement, $(a/t)_W/(a/t)_S$. This equation demonstrates that the force capacity for a "weaker" adhesive can be equal to an inherently stronger adhesive by increasing x for a given relative adhesive energy. We explore this possibility by plotting G_{CS}/G_{CW} versus $(a/t)_W/(a/t)_S$ to create an adhesion design map, which provides insight for adhesive performance,[31,32] as seen in Figure 4. In our map,

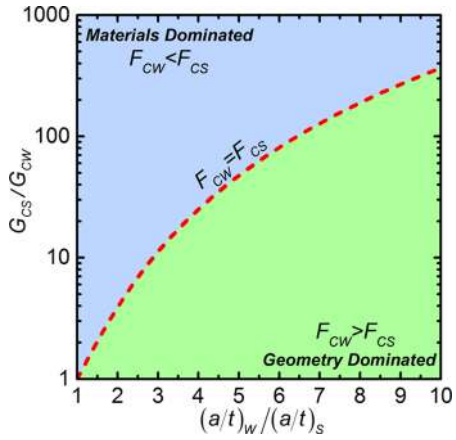

Figure 4. Adhesion design map of the relative adhesion energy versus relative confinement for a "weak" adhesive with low critical energy release rate (G_{CW}) and confinement $(a/t)_W$ and a "strong" adhesive with a high critical energy release rate (G_{CS}) and confinement $(a/t)_S$, where eq 4 is plotted with $(a/t)_S$ = 1 and represents the $F_{CW} = F_{CS}$ line. Above this line $F_{CW} < F_{CS}$ and the "strong" adhesive has a higher force capacity which is dominated by material properties. Below the line, $F_{CW} > F_{CS}$ and the "weak" adhesive achieves a higher force capacity, even with a lower adhesion energy, due to the geometric confinement of the interface.

eq 4 is plotted with $(a/t)_S$ = 1 and represents the line where equal force capacities for the "weak" and "strong" adhesives are obtained by changing the relative degree of confinement on the x-axis. Above this line $F_{CW} < F_{CS}$, where the "strong" adhesive has a higher force capacity which is dominated by material properties, while below the line $F_{CW} > F_{CS}$, and the "weak" adhesive has a higher force capacity due to the geometric confinement of the interface. For example, consider a "weak" adhesive with a low energy of release of G_{CW} = 0.1 J/m^2; eq 4 shows that this material can have the same or greater force capacity as a "strong" adhesive with G_{CS} = 10 J/m^2 and $(a/t)_S$ = 1, if the confinement of the "weak" adhesive is $(a/t)_W \geq 6.5$ (design maps for additional $(a/t)_S$ are in Figure S2 in the Supporting Information). For a constant contact size of the two adhesives, this is accomplished by decreasing the thickness of the "weak" adhesive. This map demonstrates the importance of contact geometry, specifically geometric confinement, and can be utilized to increase adhesive performance when designing for reversible or repeated use, adhering to low energy surfaces, or when utilizing materials which are not inherently "sticky" or "tacky".

To describe adhesive force capacity as a function of confinement in a more general context, we return to eq 1 which states that F_C scales as $(A/C)^{1/2}$, where A is the projected contact area of the rigid cylindrical punch and C is the measured compliance. We apply this parameter to our experimental data for all of the contact radii and substrate thicknesses investigated and find good agreement by plotting F_C versus $(A/C)^{1/2}$, as seen in Figure 5. The scaling parameter

dx.doi.org/10.1021/la4013526 | Langmuir 2013, 29, 11022−11027

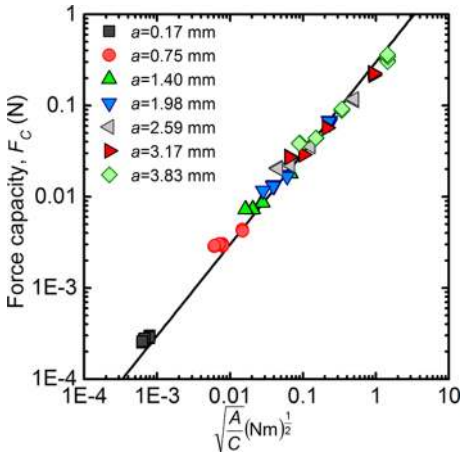

Figure 5. Log–log plot of force capacity, F_C, versus $(A/C)^{1/2}$ for all of the tested geometries, including seven rigid cylindrical punches each tested on four different substrate thicknesses, where A is the projected contact area of the rigid cylindrical punch and C is the measured compliance. The data collapses onto the solid line described by eq 1 through the A/C scaling parameter, with G_C = 0.05 J/m^2.

collapses all of these data onto a single line over orders of magnitude in adhesive force capacity. The line is plotted with a G_C value of 0.05 J/m^2, which is in good agreement with previously reported values.[15,27] Importantly, as eq 1 does not assume a specific separation mechanism or form for the compliance, the adhesive force capacity is well described during axisymmetric edge separation and for interfacial fingering and cavitation instabilities. Additionally, as A and C are experimentally assessable, measured quantities they do not require solving a contact mechanics problem or knowing them a priori. This generality provides opportunities to investigate unusual separation mechanisms and contact geometries, such as the variety of contact shapes utilized in fibrillar, bioinspired attachment features.[33−35] Additionally, the change in stress distribution under a rigid indenter as confinement is increased does not influence the prediction from the A/C scaling parameter. This understanding provides a continuous prediction of force capacity over a wide range of a/t confinement ratios through experimentally measured parameters.

CONCLUSION

In this paper, we present a continuous and robust understanding of the compliance and adhesive force capacity of a model elastic layer with varying levels of confinement. This study shows the following: (i) Compliance and force capacity are both insensitive to confinement at low a/t ratios, but depend strongly on a/t as confinement is increased. This behavior is consistent with previous reports, but the predicted continuity between low and high a/t ratios by eqs 2 and 3 has not been previously demonstrated. (ii) Controlling the a/t ratio during material testing is crucial as a small change can have a drastic influence on the measured results. This is especially relevant when the indenter radius becomes commensurate or larger than the substrate thickness. (iii) Confinement can be used as a strong design parameter for reversible adhesive interfaces. Increasing confinement can be used to enhance adhesion, enabling inherently "weak" adhesives to achieve high force capacities similar to or greater than "strong" adhesives. We present a design map to guide engineers and scientists in the future application of this concept. (iv) The adhesive force capacity of a rigid punch on an elastic substrate can be well described by the generalized A/C scaling parameter. This functions over orders of magnitude in size, confinement and force capacity, even in the presence of nonaxisymmetric debonding mechanisms.

ASSOCIATED CONTENT

Supporting Information

Adhesive force capacity results as a function of compressive preload and displacement rate (Figure S1). Adhesion design maps for additional $(a/t)_S$ (Figure S2). This material is available free of charge via the Internet at http://pubs.acs.org.

AUTHOR INFORMATION

Corresponding Author

*E-mail: Crosby@mail.pse.umass.edu.

Notes

The authors declare no competing financial interest.

ACKNOWLEDGMENTS

M.D.B. and A.J.C. acknowledge the University of Massachusetts research funds for support of this research. M.D.B. thanks S. A. Pendergraph, J. T. Pham, and D. R. King for thoughtful discussions.

REFERENCES

(1) Brady, R. F.; Singer, I. L. Mechanical factors favoring release from fouling release coatings. *Biofouling* **2000**, *15*, 73−81.
(2) Hui, C. Y.; Long, R.; Wahl, K. J.; Everett, R. K. Barnacles resist removal by crack trapping. *J. R. Soc., Interface* **2011**, *8*, 868−879.
(3) Creton, C. Pressure-sensitive adhesives: an introductory course. *MRS Bull.* **2003**, *28*, 434−439.
(4) Lin, Y. Y.; Hui, C.; Conway, H. D. A Detailed Elastic Analysis of the Flat Punch (Tack) Test for Pressure-Sensitive Adhesives. *J. Polym. Sci., Part B: Polym. Phys.* **2000**, *38*, 2769−2784.
(5) Carlson, A.; Bowen, A. M.; Huang, Y.; Nuzzo, R. G.; Rogers, J. A. Transfer printing techniques for materials assembly and micro/nanodevice fabrication. *Adv. Mater.* **2012**, *24*, 5284−5318.
(6) Hui, C. Y.; Jagota, A.; Lin, Y. Y.; Kramer, E. J. Constraints on Microcontact Printing Imposed by Stamp Deformation. *Langmuir* **2002**, *18*, 1394−1407.
(7) Ganghoffer, J.; Gent, A. Adhesion of a rigid punch to a thin elastic layer. *J. Adhes.* **1995**, *48*, 75−84.
(8) Kim, S.; Sitti, M.; Hui, C.-Y.; Long, R.; Jagota, A. Effect of backing layer thickness on adhesion of single-level elastomer fiber arrays. *Appl. Phys. Lett.* **2007**, *91*, 161905.
(9) Shull, K. R.; Creton, C. Deformation behavior of thin, compliant layers under tensile loading conditions. *J. Polym. Sci., Part B: Polym. Phys.* **2004**, *42*, 4023−4043.
(10) Tang, T.; Hui, C.-Y. Decohesion of a rigid punch from an elastic layer: Transition from "flaw sensitive" to "flaw insensitive" regime. *J. Polym. Sci., Part B: Polym. Phys.* **2005**, *43*, 3628−3637.
(11) Creton, C.; Lakrout, H. Micromechanics of flat-probe adhesion tests of soft viscoelastic polymer films. *J. Polym. Sci., Part B: Polym. Phys.* **2000**, *38*, 965−979.
(12) Shull, K. R.; Flanigan, C.; Crosby, A. J. Fingering instabilities of confined elastic layers in tension. *Phys. Rev. Lett.* **2000**, *84*, 3057−3060.
(13) Fond, C. Cavitation criterion for rubber materials: A review of void-growth models. *J. Polym. Sci., Part B: Polym. Phys.* **2001**, *39*, 2081−2096.
(14) Kendall, K. The adhesion and surface energy of elastic solids. *J. Phys. D: Appl. Phys.* **1971**, *4*, 1186−1195.
(15) Webber, R.; Shull, K. R.; Roos, A.; Creton, C. Effects of geometric confinement on the adhesive debonding of soft elastic solids. *Phys. Rev. E: Stat., Nonlinear, Soft Matter Phys.* **2003**, *68*, 021805.

(16) Maugis, D.; Barquins, M. Fracture mechanics and the adherence of viscoelastic bodies. *J. Phys. D: Appl. Phys.* **1978**, *11*, 1989−2023.
(17) Chung, J. Y.; Chaudhury, M. K. Soft and Hard Adhesion. *J. Adhes.* **2005**, *81*, 1119−1145.
(18) Yang, F.; Li, J. C. M. Adhesion of a Rigid Punch to an Incompressible Elastic Film. *Langmuir* **2001**, *17*, 6524−6529.
(19) Johnson, K.; Kendall, K.; Roberts, A. Surface energy and the contact of elastic solids. *Proc. R. Soc. London, Ser. A* **1971**, *324*, 301−313.
(20) Maugis, D. Adhesion of spheres: The JKR-DMT transition using a dugdale model. *J. Colloid Interface Sci.* **1992**, *150*, 243−269.
(21) Crosby, A. J.; Shull, K. R.; Lakrout, H.; Creton, C. Deformation and failure modes of adhesively bonded elastic layers. *J. Appl. Phys.* **2000**, *88*, 2956−2966.
(22) Sarkar, J.; Shenoy, V.; Sharma, A. Patterns, Forces, and Metastable Pathways in Debonding of Elastic Films. *Phys. Rev. Lett.* **2004**, *93*, 018302.
(23) Shenoy, V.; Sharma, A. Pattern Formation in a Thin Solid Film with Interactions. *Phys. Rev. Lett.* **2001**, *86*, 119−122.
(24) Ghatak, A.; Chaudhury, M.; Shenoy, V.; Sharma, A. Meniscus instability in a thin elastic film. *Phys. Rev. Lett.* **2000**, *85*, 4329−4332.
(25) Bartlett, M. D.; Croll, A. B.; King, D. R.; Paret, B. M.; Irschick, D. J.; Crosby, A. J. Looking Beyond Fibrillar Features to Scale Gecko-Like Adhesion. *Adv. Mater.* **2012**, *24*, 1078−1083.
(26) Bartlett, M. D.; Croll, A. B.; Crosby, A. J. Designing Bio-Inspired Adhesives for Shear Loading: From Simple Structures to Complex Patterns. *Adv. Funct. Mater.* **2012**, *22*, 4985−4992.
(27) Mowery, C.; Crosby, A.; Ahn, D.; Shull, K. Adhesion of thermally reversible gels to solid surfaces. *Langmuir* **1997**, *7463*, 6101−6107.
(28) Paretkar, D. R.; Bartlett, M. D.; McMeeking, R.; Crosby, A. J.; Arzt, E. Buckling of an Adhesive Polymeric Micropillar. *J. Adhes.* **2013**, *89*, 140−158.
(29) Kroner, E.; Blau, J.; Arzt, E. An adhesion measurement setup for bioinspired fibrillar surfaces using flat probes. *Rev. Sci. Instrum.* **2012**, *83*, 016101D.
(30) Shull, K. R.; Ahn, D.; Chen, W. L.; Flanigan, C. M.; Crosby, A. J. Axisymmetric adhesion tests of soft materials. *Macromol. Chem. Phys.* **1998**, *199*, 489−511.
(31) Spolenak, R.; Gorb, S.; Arzt, E. Adhesion design maps for bio-inspired attachment systems. *Acta Biomater.* **2005**, *1*, 5−13.
(32) Greiner, C.; Spolenak, R.; Arzt, E. Adhesion design maps for fibrillar adhesives: the effect of shape. *Acta Biomater.* **2009**, *5*, 597−606.
(33) Spolenak, R.; Gorb, S.; Gao, H.; Arzt, E. Effects of contact shape on the scaling of biological attachments. *Proc. R. Soc. A* **2005**, *461*, 305−319.
(34) Del Campo, A.; Greiner, C.; Arzt, E. Contact shape controls adhesion of bioinspired fibrillar surfaces. *Langmuir* **2007**, *23*, 10235−10243.
(35) Chan, E. P.; Greiner, C.; Arzt, E.; Crosby, A. J. Designing Model Systems for Enhanced Adhesion. *MRS Bull.* **2007**, *32*, 496−503.